Hindawi Publishing Corporation
Mathematical Problems in Engineering
Volume 2015, Article ID 315898, 9 pages
http://dx.doi.org/10.1155/2015/315898

Research Article

A Novel SHMPWM Technique for Sensorless Control in High-Power PMSM

Yanjun Yu, Lixiao Gao, Yue Liu, Feng Chai, and Shukang Cheng

School of Electrical Engineering and Automation, Harbin Institute of Technology, Harbin 150001, China

Correspondence should be addressed to Yanjun Yu; yuyanjun@hit.edu.cn

Received 28 July 2014; Revised 16 January 2015; Accepted 29 January 2015

Academic Editor: Mehmet Onder Efe

In view of the low switching frequency restriction of high-power permanent magnet synchronous motor (PMSM) drive system and longing for sensorless control in hostile conditions, a novel PWM control scheme, born out of selective harmonic mitigation pulse width modulation (SHMPWM) technique, was proposed for sensorless control of high-power PMSM. A new enhanced constraint was placed on the traditional SHMPWM nonlinear transcendental equation to selectively generate constant amount of a certain $3k+1$ order harmonic signals while guaranteed that the undesired harmonic signals can be suppressed. At the same time, the $3k+1$ order harmonic signals were extracted by band-pass filter, which had the constant amplitude and phase angle difference of 120°, equivalent to inject rotating voltage vector in the natural coordinate system of motor, and the rotor position can be estimated using the $3k+1$ order harmonic signals. The nonlinear transcendental equation of the novel modulation technique had been designed, and its numerical method had been analyzed. The rotor position observer had been designed according to the $3k+1$ order harmonic signals. Simulation results verify that the harmonic suppression of the system was implemented, and the sensorless control was efficient by the novel SHMPWM technique.

1. Introduction

High-power permanent magnet synchronous motor (PMSM) has a wide range of applications in electric drive system such as electric vehicle and high-speed rail due to its design philosophy of high efficiency and energy conservation [1].

On the one hand, the high-power motor drive system is more technically required in many aspects than the drive system of medium and low power. From the perspective of the inverters, the highest switching frequency is a few hundred Hz because of the limitation caused by switching loss and heat dissipation. Whereas the fundamental frequency of the electrical machines sometimes approaches to 200 Hz and even higher, the decrease in the switching frequency will increase the harmonic components in the system. If the conventional pulse width modulation (PWM) is still used, then a large-sized filter circuit is supposed to be connected to the main transform circuit to meet the requirement of the system. However, this will upsize the system, reduce the efficiency of the inverters, and increase the cost greatly. Therefore, specific control strategies should be taken, for example, the selective harmonic elimination pulse width modulation (SHEPWM) or the selective harmonic mitigation pulse width modulation (SHMPWM), so as to reduce the harmonic components, downsize the system, and improve the efficiency of the whole system [2–4].

On the other hand, it is necessary to obtain the information about the rotor's position and velocity in order to achieve a better performance control on the high-power PMSMs. This is usually realized by mechanical sensors such as the encoders and resolvers. However, the assembly of the mechanical sensors will bring about a large number of problems such as increasing the cost, decreasing the reliability, upsizing the system, and reducing the anti-interference ability. The sensorless control is a hot spot in the high performance machine driving field aimed at widening the application range of the PMSMs. The control strategies of the sensorless control are mainly divided into two types: fundamental magnetizing method and high-frequency signal component method. The former is based on the fundamental

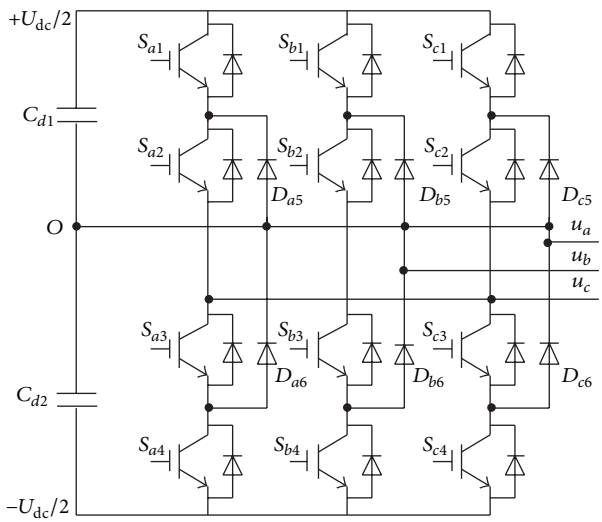

Figure 1: Three-level NPC inverter topology.

dynamic model of the electrical machine [5, 6] and suitable for sensorless operation at a medium or high speed. The latter is based on the space-saliency effect and the rotor position is observed simultaneously by injecting high-frequency excitation signal into the electrical machine so that the sensorless operation of the IPMSMS can be realized at the overall speed range. Thus, the sensorless control of the IPMSMs based on the high-frequency component model is of great practical significance [7–9]. However, in the high-power PMSM drive system, if the specific high-frequency is obtained by injecting an external signal, it will be difficult to select the frequency of the injecting signal as the difference between the fundamental frequency of the electrical machine and the switching frequency is quite small.

This paper proposes a novel SHMPWM technique for sensorless control in high-power PMSMs considering the working condition. The SHMPWM technique is used to reduce the main harmonic components of low order in the system. Moreover, a new enhanced constraint was placed on the traditional SHMPWM nonlinear transcendental equation to generate harmonic signal of specific order to estimate the rotor position. By this way the rotor position can be obtained without injecting any specific external signal. The simulation analysis of the system has also been done and the results have proven the correctness and effectiveness of the proposed control algorithm.

2. Novel SHMPWM Technique Principle

2.1. The Harmonic Analysis on the Three-Level Inverter. In this paper, three-level NPC inverter for high-power PMSM system is used and its topology is shown in Figure 1.

The output voltage waveform of the three-level NPC inverter is illustrated in Figure 2. Assume that there are N switching angles in the $[0, \pi/2]$ period; α_i $(i = 1, 2, \ldots, N)$ represents the switching angle.

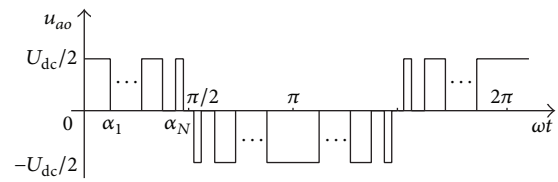

Figure 2: Three-level PWM switch mode of the inverter.

The waveform which is given in Figure 2 can be expressed as (1) by Fourier Series expansion

$$f(x) = a_0 + \sum_{j=1}^{\infty} \left[a_j \cos(jx) + b_j \sin(jx)\right], \tag{1}$$

where

$$\begin{aligned} a_0 &= \frac{1}{\pi}\int_0^{2\pi} f(x)\,dx, \\ a_j &= \frac{1}{\pi}\int_0^{2\pi} f(x)\cos(jx)\,dx, \\ b_j &= \frac{1}{\pi}\int_0^{2\pi} f(x)\sin(jx)\,dx. \end{aligned} \tag{2}$$

From Figure 2, as $f(x)$ is 1/2 and 1/4 periodic symmetric, then

$$\begin{aligned} a_0 &= \frac{1}{\pi}\int_0^{2\pi} f(x)\,dx = 0, \\ a_j &= \frac{4U_{dc}}{j\pi}\sum_{i=1}^{N}\left[(-1)^{i+1}\sin(j\alpha_i)\right], \\ b_j &= \frac{1}{\pi}\int_0^{2\pi} f(x)\sin(jx)\,dx = 0, \end{aligned} \tag{3}$$

where $j = 5, 7, 11, \ldots$.

From (3), the ratio of the amplitude of j order harmonic component and DC-bus voltage is

$$H_j = \frac{4}{j\pi}\sum_{i=1}^{N}\left[(-1)^{i}\sin(j\alpha_i)\right]. \tag{4}$$

2.2. SHMPWM Modulation Algorithm. The classic SHEPWM technique fixes the value of H_1 (which is normally called the modulation index (M_a)) and also eliminates $N-1$ harmonics; the nonlinear transcendental equation can be written as

$$\begin{aligned} H_1 &= \frac{4}{\pi}\sum_{i=1}^{N}\left[(-1)^{i+1}\sin(a_i)\right], \\ 0 &= \frac{4}{j\pi}\sum_{i=1}^{N}\left[(-1)^{i+1}\sin(ja_i)\right]. \end{aligned} \tag{5}$$

The SHMPWM is not aimed at eliminating the harmonic components of specific orders to zero but keeping them

within their allowable ranges of a related standard; the nonlinear transcendental equation can be written as [4]

$$\begin{gathered}\left|M_a - H_1\right| \le L_1 \\ \frac{1}{\left|H_1\right|}\frac{4}{j\pi}\sum_{i=1}^{N}\left[(-1)^{i+1}\sin\left(ja_i\right)\right] \le L_j,\end{gathered} \tag{6}$$

where M_a is the modulation index and L_j is the maximum limit of jth harmonic component.

2.3. A Novel SHMPWM Technique. Equation (6) can only be used to suppress the harmonics of the system. However, it cannot be used to generate the high-frequency signal by which the rotor position can be estimated. In order to realize the sensorless control on the electrical machine, the constraint on (6) is enhanced and a novel SHMPWM nonlinear transcendental equation is obtained so that the amplitude of a certain order harmonic is kept constant by the premise of satisfying the allowable ranges of a related standard; the constraint is as follows:

$$\begin{gathered}\left|M_a - H_1\right| \le L_1, \\ \frac{1}{\left|H_1\right|}\frac{4}{j\pi}\sum_{i=1}^{N}\left[(-1)^{i}\sin\left(ja_i\right)\right] \le L_j, \\ \frac{1}{\left|H_1\right|}\frac{4}{m\pi}\sum_{i=1}^{N}\left[(-1)^{i}\sin\left(ma_i\right)\right] = L_m,\end{gathered} \tag{7}$$

where $j = 5, 7, 9, \ldots, m-2, m+2, \ldots$, and m represents the specific harmonic order of the signal which is used to realize the sensorless control.

Equation (7) on the one hand guarantees that the harmonics of the system are limited within an approved harmonic range so that the harmonics of the system are suppressed effectively; on the other hand, the amplitude of mth order harmonic is kept constant to meet the requirement in sensorless control.

A phase difference of 120° from each other is required for the 3-phase specific order harmonics in sensorless control; the 3-phase mth order harmonic of the inverter output voltage can be expressed by Fourier analysis as follows:

$$\begin{aligned}u_{am} &= H_m \sin\left(m\omega t\right), \\ u_{bm} &= H_m \sin\left(m\omega t - m\times 120^\circ\right), \\ u_{cm} &= H_m \sin\left(m\omega t + m\times 120^\circ\right).\end{aligned} \tag{8}$$

If $m = 3k+1$, $k = 1, 2, 3, \ldots$, (8) can be expressed as

$$\begin{aligned}u_{am} &= H_m \sin\left(m\omega t\right), \\ u_{bm} &= H_m \sin\left(m\omega t - k\times 360^\circ - 120^\circ\right) \\ &= H_m \sin\left(m\omega t - 120^\circ\right), \\ u_{cm} &= H_m \sin\left(m\omega t + k\times 360^\circ + 120^\circ\right) \\ &= H_m \sin\left(m\omega t + 120^\circ\right).\end{aligned} \tag{9}$$

From (9), it can be concluded that when the selected specific harmonic order $m = 3k+1$, $k = 1, 2, 3, \ldots$, the phase difference between the selected 3-phase harmonics is 120°, which meet the requirement in sensorless control. Namely, the harmonics of 7th, 13th, 19th, and 25th order can be selected to be used as the specific signal components to estimate the rotor position.

The nonlinear transcendental equation of the proposed novel SHMPWM technique can also be derived via (7) if $m = 3k+1$, $k = 1, 2, 3, \ldots$.

3. The Numerical Solution of the Novel SHMPWM

Equation (7) can be solved by the conventional Newton-Raphson Iteration which is more applicable for equalities than inequalities. Furthermore, the Newton-Raphson method depends highly on the choice of the initial value. An unsuitable initial value may cause difficulties and even divergence in the iteration process. Thus, the optimization method is used in this paper to solve the SHMPWM equation.

When $N = 5$ and the harmonic components of less than 50th order are suppressed, the equations of the SHMPWM algorithm are analyzed. Equation (7) is equivalent to

$$\begin{aligned}&\min \quad \mathrm{THD}_{50} \\ &\text{s.t.} \quad M_a - \left|H_1\right| \le L_1 \\ &\qquad \frac{1}{\left|H_1\right|}\frac{4}{m\pi}\sum_{i=1}^{5}\left[(-1)^{i+1}\sin\left(m\alpha_i\right)\right] = L_m \\ &\qquad \frac{1}{\left|H_1\right|}\frac{4}{j\pi}\sum_{i=1}^{5}\left[(-1)^{i+1}\sin\left(m\alpha_i\right)\right] \le L_j,\end{aligned} \tag{10}$$

where THD_{50} is the total harmonic distortion of the top 50 orders and $H_1 = (4/\pi)\sum_{i=1}^{5}[(-1)^{i+1}\sin(\alpha_i)]$. Let $L_1 = 0$, namely, $M_a = H_1$. And the specific harmonic order m is chosen as $m = 25$. Then (10) can be written as follows:

$$\begin{aligned}&\min \quad f(X) = \mathrm{THD}_{50}(X) \\ &\text{s.t.} \quad h_1(X) = M_a - \frac{4}{\pi}\sum_{i=1}^{5}\left[(-1)^{i+1}\sin\left(x_i\right)\right] = 0 \\ &\qquad h_2(X) = L_{25} - \frac{1}{\left|H_1\right|}\frac{4}{25\pi}\sum_{i=1}^{5}\left[(-1)^{i+1}\sin\left(25x_i\right)\right] = 0 \\ &\qquad g_j(X) = L_j - \frac{1}{\left|H_1\right|}\frac{4}{j\pi}\sum_{i=1}^{5}\left[(-1)^{i+1}\sin\left(mx_i\right)\right] \ge 0,\end{aligned} \tag{11}$$

where $g_j(X)$ is the harmonic constraint whose amplitude should be limited, $j = 5, 7, \ldots, 47, 49$. All of $f(X)$, $h_i(X)$, and $g_j(X)$ possess continuous partial derivatives of first order.

Penalty function method is used to construct objective function OF as follows, and it is assumed that N numbers of

inequality constraints are added to the constraint equation of SHMPWM:

$$\mathrm{OF}\left(X, m_i, m_j\right) = f(X) + \sum_{i=1}^{2} m_i \left[h_i(X)\right]^2 + \sum_{j=1}^{n} m_j \left[g_j(X)\right]^2 u_j\left(g_j\right), \tag{12}$$

where $u_j(g_j)$ is the nonlinear function which is deliberately introduced aimed at creating an easier access to solve the equation; it can be expressed as

$$u_j\left(g_j\right) = \begin{cases} 0, & \text{if } g_j \geq 0 \\ 1, & \text{if } g_j < 0, \end{cases} \tag{13}$$

where m_i, m_j represent the penalty factor; additionally, $m_i, m_j \gg 1$.

The function of $u_j(g_j)$ is that if g_j satisfies the inequality constraint, then u_j is set to 0; that is, g_j has no effect on the objective function OF; if g_j does not satisfy the inequality constraint, then u_j is set to 1, so the product of g_j and penalty factor makes the value of the objective function OF rise rapidly. The optimization problems with constraints have been transformed to optimization problems without constraints by changing the constraints of the SHMPWM equation which is realized via setting the value of $u_j(g_j)$. Moreover, $u_j(g_j)$ enlarges the difference between function values when the independent variables are chosen from the feasible and infeasible solutions area in the solution space of the SHMPWM constraint equation, which plays a role of constraint so the correctness of the solution is guaranteed. The effect of different subfunctions on the objective function OF as well as the weight of different harmonics can be changed by modifying the value of the penalty factor; in this way the promising result is flexibly controlled. Additionally, as arbitrary number of inequality constraints can be applied to the equation, that is, the limitations on the amplitude of arbitrary number of harmonics can be set, the feature that the SHMPWM can only control the amplitude of a limited number of harmonics vanishes so that the output harmonics can be better controlled. The problem of solving the SHMPWM nonlinear transcendental equation has been transformed into the problem of determining the minimum value of the objective function OF after the construction of objective function OF. Meanwhile, the optimization problem with constraint has been transformed to that without constraint, which simplifies the solving process greatly.

In the solving process, two equality constraints, that is, the equality constraints on the amplitude of fundamental and 25th order harmonic, respectively, are introduced to balance the rapidity and accuracy in the solving process with the requirement of generating rotating voltage vector of specific component. The feasible solutions under different modulation ratio M_a can be determined by putting equality constraint on different amplitudes of the fundamental frequency (the modulation ratio M_a).

When $M_a = 0.9$ and $L_{25} = 0.15$, the feasible solutions are as follows: $X_2 = [0.61651\ 0.70418\ 0.81797\ 1.00941\ 1.08123]$.

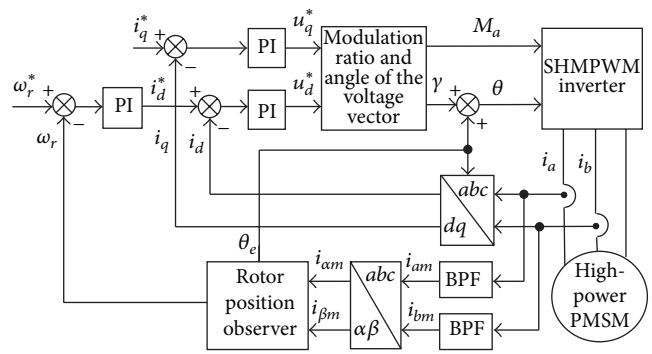

Figure 3: The schematic diagram of PMSM close loop control system based on SHMPWM.

4. The High-Power PMSM Sensorless Vector Control System Based on SHMPWM Technique

4.1. The System Construction. As the SHMPWM technique regards all the switching actions in one period as one action, the current of the electrical machine cannot be controlled in real time by controlling the individual switching action, so special strategy is needed to complete the vector close loop of the electrical machines. The schematic diagram of the PMSM close loop control system based on SHMPWM is given in Figure 3.

In Figure 3, BPF is the band-pass filter. When the driver system is implemented, 50-order FIR filters are used for the digital filtering of the phase-current signals, and then the mth order harmonic current signals can be obtained from BPF. The cut-off frequency selection of the FIR filters is difference of about 10 octaves for signal sampling frequency. The bandwidth is narrower, the achieved mth order harmonic current signals are more accurate, the estimated rotor position error is smaller, and this leads the system to have high dynamic or steady performance.

The vector control can be realized by regulating the modulation ratio M_a and the phase of voltage vector θ in the SHMPWM output waveform.

From the Park inverse transform matrix

$$\begin{bmatrix} u_\alpha \\ u_\beta \end{bmatrix} = \begin{bmatrix} \cos\theta_e & -\sin\theta_e \\ \sin\theta_e & \cos\theta_e \end{bmatrix} \begin{bmatrix} u_d \\ u_q \end{bmatrix}, \tag{14}$$

where θ_e is the rotor angle at the current position. Trigonometric transform is carried on (14) and the result is

$$\begin{aligned} u_\alpha &= \sqrt{u_d^2 + u_q^2}\cos\left(\theta_e + \gamma\right), \\ u_\beta &= \sqrt{u_d^2 + u_q^2}\sin\left(\theta_e + \gamma\right), \end{aligned} \tag{15}$$

where γ is the calculated angle whose value is determined by

$$\gamma = \arctan\frac{u_q}{u_d}. \tag{16}$$

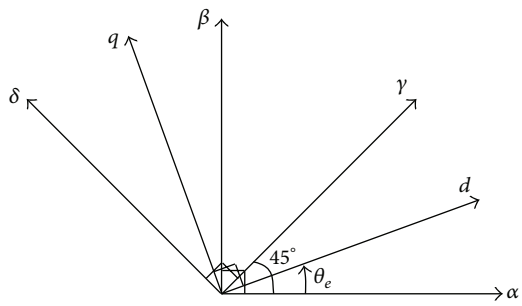

Figure 4: Space-vector diagram for rotor position estimation.

The voltage vector θ of a-phase is determined by

$$\theta = \theta_e + \gamma. \tag{17}$$

The phase of voltage vector of b- and c-phase can be acquired by delaying the phase of voltage vector of a-phase by 120° and 240°, respectively.

The modulation index M_a can be obtained directly by (15) and the correlation between the amplitude of sine wave and square wave

$$M_a = \frac{\pi}{\sqrt{6}} \frac{\sqrt{u_d^2 + u_q^2}}{U_{\mathrm{dc}}}. \tag{18}$$

4.2. Rotor Positions Estimation Principle Using Rotating Voltage Vector Signals. In order the determine the formula which can be used to estimate the rotor position, two 2-phase static reference coordinates are built and their space-vector correlation is shown in Figure 4 [9].

Based on the high-frequency mathmatic models and coordinate transformation theory, the equation of the current envelop of mth order harmonic under α-β and γ-δ frames of high-power PMSM can be determined from (9)

$$\begin{aligned}
\begin{bmatrix} |i_{\alpha m}|_{\mathrm{peak}} \\ |i_{\beta m}|_{\mathrm{peak}} \end{bmatrix} &= \frac{3 \times H_m}{2 \times m\omega \left(L_0^2 - L_1^2\right)} \\
&\quad \cdot \begin{bmatrix} \sqrt{L_0^2 + L_1^2 + 2L_0L_1 \cos\left(2\theta_e\right)} \\ \sqrt{L_0^2 + L_1^2 - 2L_0L_1 \cos\left(2\theta_e\right)} \end{bmatrix}, \\
\begin{bmatrix} |i_{\gamma m}|_{\mathrm{peak}} \\ |i_{\delta m}|_{\mathrm{peak}} \end{bmatrix} &= \frac{3 \times H_m}{2 \times m\omega \left(L_0^2 - L_1^2\right)} \\
&\quad \cdot \begin{bmatrix} \sqrt{L_0^2 + L_1^2 + 2L_0L_1 \sin\left(2\theta_e\right)} \\ \sqrt{L_0^2 + L_1^2 - 2L_0L_1 \sin\left(2\theta_e\right)} \end{bmatrix},
\end{aligned} \tag{19}$$

where L_0 represents the average value of the inductance, $L_0 = (L_d + L_q)/2$; L_1 stands for the half of the difference between L_d and L_q, namely, $L_1 = (L_d - L_q)/2$, L_d, L_q represent the d-axis inductance and q-axis inductance, respectively, and θ_e is the rotor position in electrical degree.

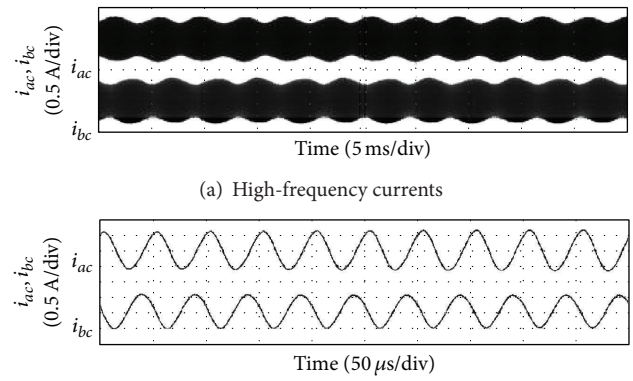

(a) High-frequency currents

(b) Enlarged drawing of high-frequency currents

Figure 5: Experimental results of the high-frequency current signals by BPF.

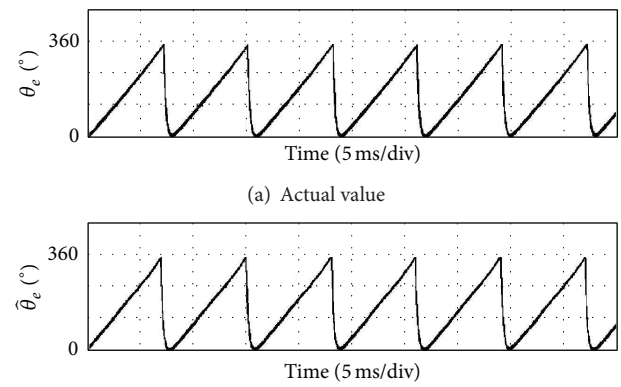

(a) Actual value

(b) Estimated value

Figure 6: Estimated and actual results of the rotor position.

The information of the rotor position is included in $\cos(2\theta_e)$ and $\sin(2\theta_e)$ in (19); from the law of cosines, the formula of the rotor position estimation can be determined as

$$\hat{\theta}_e = \frac{1}{2}\tan^{-1}\left(\frac{|i_{\gamma c}|_{\mathrm{peak}}^2 - |i_{\delta c}|_{\mathrm{peak}}^2}{|i_{\alpha c}|_{\mathrm{peak}}^2 - |i_{\beta c}|_{\mathrm{peak}}^2}\right). \tag{20}$$

The described design methods for band-pass filter and rotor position observer have been realized in the 200 W IPMSM sensorless control system based on the carrier frequency component method and two-level inverter [10, 11]. The experimental results are shown in Figures 5–7. Figure 5 shows that the designed BPF is correct, and Figures 6 and 7 show that the designed rotor position observer is feasible. The experimental results demonstrate the design methods for band-pass filter and rotor position observer are reasonable and feasible. These methods can also be applied in high-power PMSM sensorless control using the novel SHMPWM technique.

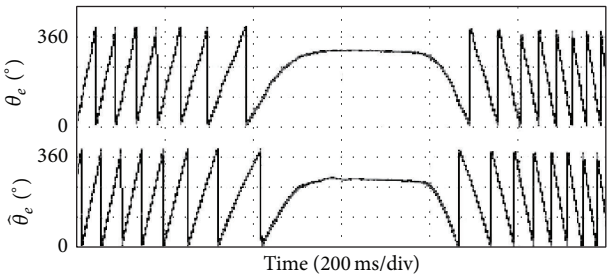

Figure 7: Actual and estimated rotor position when speed is reversed.

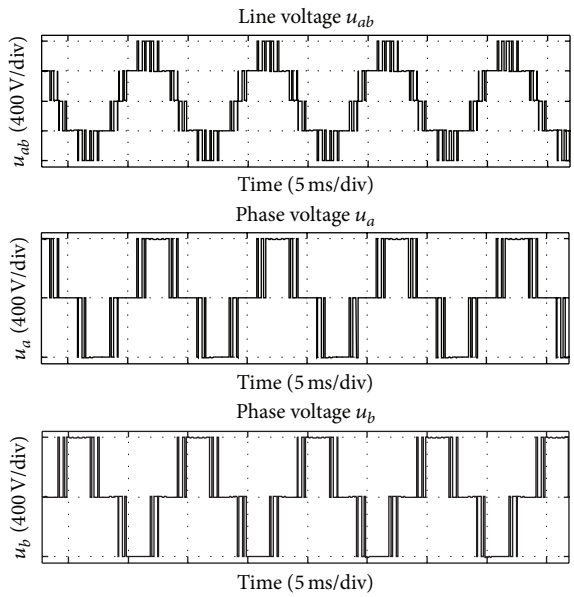

Figure 8: The waveforms of the inverter output line voltage u_{ab} and phase voltages u_a and u_b under SHMPWM.

5. Simulation Results

In order to prove the correctness of the proposed algorithm, the model of the system based on Matlab/Simulink is built and the simulation analysis is implemented. The key parameters of the system are given in Table 1.

Figure 8 shows the waveforms of the inverter output line voltage u_{ab} and phase voltages u_a, u_b under the SHMPWM.

Figure 9 shows the waveforms of the inverter output line voltages u_{ab}, u_{bc}, and u_{ca} under SHMPWM. And Figure 10 illustrates the Fourier analysis result of inverter output line voltage u_{ab} under SHMPWM.

From the result of Fourier analysis, the maximum value of the harmonics as well as the THD decreases when SHMPWM is used at the working condition with a 500 Hz switching frequency and a 100 Hz operation frequency. The total harmonic content satisfies the approved harmonic operation range regulated by IEEE 519–1992 standard.

In order to prove the effectiveness of the proposed SHMPWM technique and the optimization method, the harmonic components calculated by the SHMPWM technique, the novel SHMPWM technique based on Newton-Raphson method, and the novel SHMPWM technique based on optimization method, respectively, are compared; the results are shown in Table 2.

Table 1: System parameters.

Parameters	Values
Rated power	200 [kW]
Switching frequency	500 [Hz]
Operation frequency	100 [Hz]
Bus voltage	800 [V]
Rated speed	1500 [r/min]
d-axis inductance	0.65 [mH]
q-axis inductance	1.95 [mH]
Number of pole pairs	4

Table 2: The comparison of the simulation harmonic content under different modulation technique.

Harmonic order	SHEMPWM (%)	SHMPWM (%) (Newton-Raphson method)	SHMPWM (%) (optimization method)
5	0.49	6.19	5.85
7	0.20	4.82	4.88
11	0.14	3.31	3.38
13	0.11	3.18	2.93
17	13.72	21.78	9.84
19	24.08	1.51	5.32
23	27.31	4.62	12.91
25	2.26	21.80	18.00
29	1.27	7.15	10.14
31	1.61	6.77	5.87
35	5.25	7.97	5.48
37	8.60	0.43	5.55
41	2.54	1.69	8.36
43	4.97	1.84	8.46
47	1.44	0.31	0.28
49	7.03	0.19	2.78
$THD_{50\text{-Tot}}$	41.32	34.97	32.06

From Table 2, (1) although the 5th and 13th order harmonics can be eliminated using SHEPWM when there are 5 switching angles, the amplitude of several harmonics achieves a high value because this method brings no limitation on the higher order harmonics. The amplitude of the 17th, 19th, and 23rd order harmonics even approaches to 30% which is far larger than that of any other harmonics, causing difficulties in filtering. (2) When the results are derived from the SHMPWM technique based on Newton-Raphson method, though low order harmonics with small amplitude are generated, the higher order harmonics are eliminated which result in a decrease in the total harmonic distortion of the top 50 order harmonics $THD_{50\text{-To}}$. The amplitude of the 5th and 13th order harmonics is so small that it can be output directly without connecting a filter. However, its performance on the control

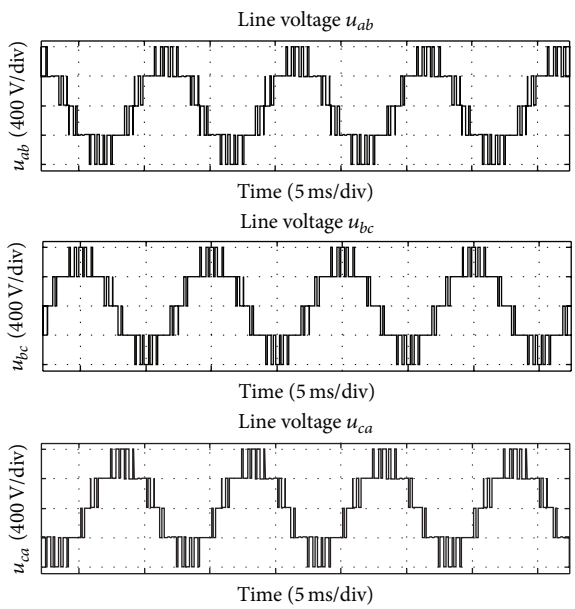

FIGURE 9: The waveforms of the inverter output line voltages u_{ab}, u_{bc}, and u_{ca} under SHMPWM.

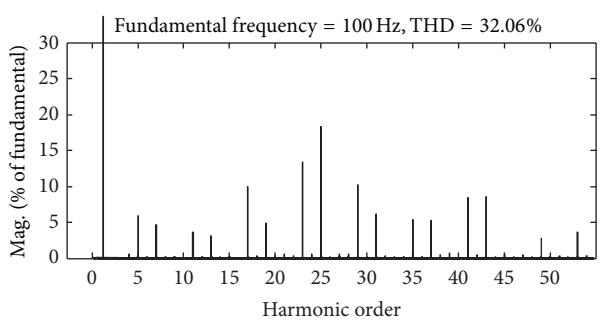

FIGURE 10: The Fourier analysis result of inverter output line voltage u_{ab} under SHMPWM.

of low order harmonic is still nonideal, because the amplitude of the 17th and 25th order harmonics is still high. As the 25th order harmonic is the high-frequency signal needed to be injected to control the system, it is supposed to be filtered out using a band-stop filter, which causes difficulties in the design process. (3) When the results are derived from the SHMPWM technique based on optimization method, the total harmonic distortion $\mathrm{THD}_{50\text{-Tot}}$ reduces significantly and the lower order harmonics are moved to higher order by the additional constraint which lead to a decrease in the amplitude of the low order harmonics. The amplitude of the 23rd order harmonics calculated by this method is no more than half of that calculated by the SHEPWM method, the amplitude of the 19th order harmonic is only 20% of which calculated by the SHEPWM method, and the amplitude of 25th order harmonic keeps unchanged so that it can be used as the high-frequency injecting signal for the sensorless control in high-power PMSM. Moreover, the higher order harmonics can be filtered out by setting a low-pass filter and even output directly without filters.

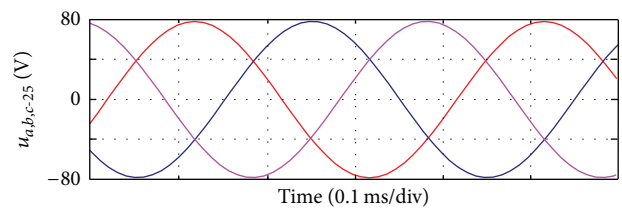

FIGURE 11: The 25th order harmonic voltage waveform in SHMPWM.

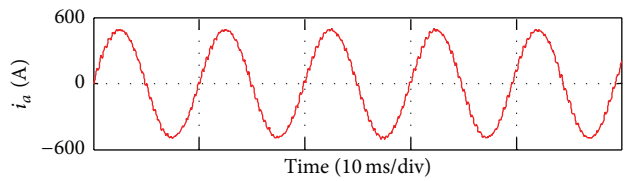

(a) a-phase stator current (i_a)

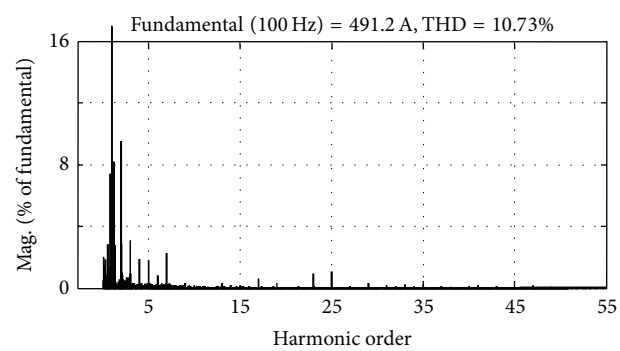

(b) The Fourier analysis result of i_a

FIGURE 12: a-phase stator current waveform and its Fourier analysis result.

Figure 11 presents the waveforms of the 25th order harmonic voltages; they have constant amplitude and a phase difference of 120°; it can be used to achieve the estimation of the rotor position.

The detailed simulation analysis has been done under rated-load test. Figure 12 shows a-phase stator current waveforms and the Fourier analysis result of the current. The current contains the 25th order harmonic current component; it can be used to estimate the rotor position of PMSM.

The response curves of speed shown from Figures 13–15 present the simulation results of the estimated rotor position and the estimated error, respectively, using the specific 25th harmonic components. The simulation results show that the information of the rotor position can be estimated accurately using the specific 25th order harmonic components, and the designed system has high dynamic and steady-state performance.

6. Conclusions

Based on the above analysis, the SHMPWM technique for sensorless control of high-power PMSM has been proposed and tested by simulations.

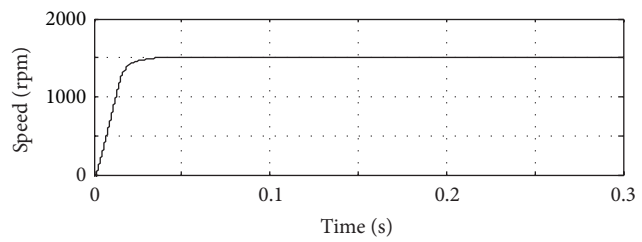

(a) 1500 rpm

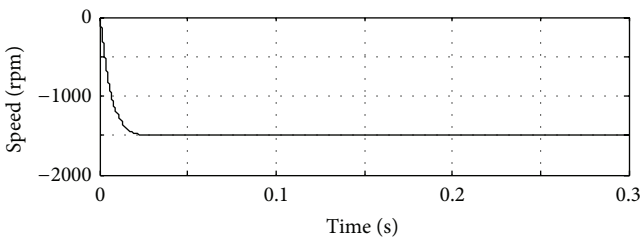

(b) −1500 rpm

Figure 13: The response curves of speed.

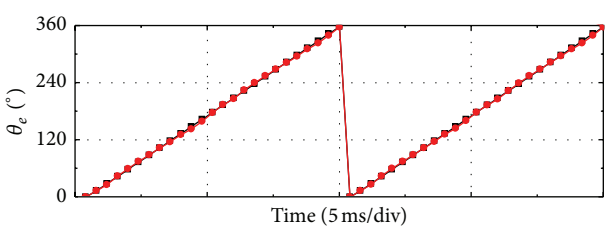

(a) Estimated rotor position

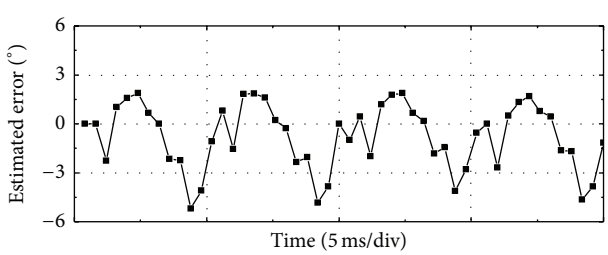

(b) Estimated error

Figure 14: The simulation results under 1500 rpm and rated-load test.

(1) By limiting the specific order harmonic in the SHMPWM constraint to a constant value, the harmonics of the system can be eliminated and the selective voltage signal of specific orders can be generated. The nonlinear transcendental equation of SHMPWM is analyzed mathematically and then the universal solving process is given by optimization method.

(2) The utilization of SHMPWM technique and the reasonable addition of the constraints to the SHMPWM equation result in a great decrease in the maximum value of the output voltage harmonics as well as the THD at the cost of increasing proportion of the low order harmonics by a small amount. The simulation results indicate that harmonic proportion in the output voltage can be 10% less than the SHEMPWM technique with the same switching angle by setting the constraint of the SHMPWM equation reasonably.

(3) By enhancing the constraints on the SHMPWM, the rotating voltage vector of 25th order which is generated by the inverters has constant amplitude and a phase difference of 120° so the sensorless control of the high-power PMSM is realized. The simulation results have proven the feasibility of the theoretical analysis.

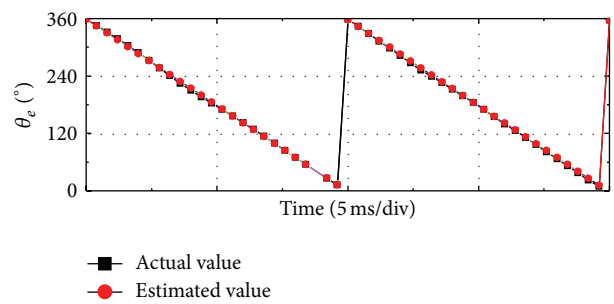

(a) Estimated rotor position

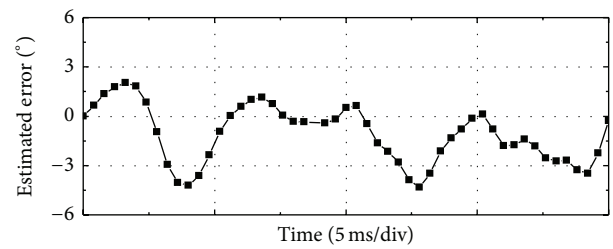

(b) Estimated error

Figure 15: The simulation results under −1500 rpm and rated-load test.

The novel SHMPWM technique proposed in this paper provides a new way in the suppression of harmonics and sensorless control in the high-power PMSM. After the theoretical analysis and simulations, the experiments on the system and research on the practical engineering are the subsequent issues to be researched.

Conflict of Interests

The authors declare that there is no conflict of interests regarding the publication of this paper.

Acknowledgments

This research was supported in part by the National Natural Science Foundation of China under Project 51307032, in part by the National Natural Science Foundation of China under Project 51477032, and in part by Research Fund for the Doctoral Program of Higher Education of China under Project 20122302120016.

References

[1] T. Noguchi, "Trends of permanent-magnet synchronous machine drives," *IEEJ Transactions on Electrical and Electronic Engineering*, vol. 2, no. 2, pp. 125–142, 2007.

[2] A. Kavousi, B. Vahidi, R. Salehi, M. K. Bakhshizadeh, N. Farokhnia, and S. H. Fathi, "Application of the bee algorithm for selective harmonic elimination strategy in multilevel inverters," *IEEE Transactions on Power Electronics*, vol. 27, no. 4, pp. 1689–1696, 2012.

[3] Y. Zhang, Z. Zhao, and J. Zhu, "A hybrid PWM applied to high-power three-level inverter-fed induction-motor drives," *IEEE Transactions on Industrial Electronics*, vol. 58, no. 8, pp. 3409–3420, 2011.

[4] J. Napoles, J. I. Leon, R. Portillo, L. G. Franquelo, and M. A. Aguirre, "Selective harmonic mitigation technique for high-power converters," *IEEE Transactions on Industrial Electronics*, vol. 57, no. 7, pp. 2315–2323, 2010.

[5] C. French and P. Acarnley, "Control of permanent magnet motor drives using a new position estimation technique," *IEEE Transactions on Industry Applications*, vol. 32, no. 5, pp. 1089–1097, 1996.

[6] Y.-S. Han, J.-S. Choi, and Y.-S. Kim, "Sensorless PMSM drive with a sliding mode control based adaptive speed and stator resistance estimator," *IEEE Transactions on Magnetics*, vol. 36, no. 5, pp. 3588–3591, 2000.

[7] S. Bolognani, S. Calligaro, R. Petrella, and M. Tursini, "Sensorless control of IPM motors in the low-speed range and at standstill by HF injection and DFT processing," *IEEE Transactions on Industry Applications*, vol. 47, no. 1, pp. 96–104, 2011.

[8] Y.-S. Jeong, R. D. Lorenz, T. M. Jahns, and S.-K. Sul, "Initial rotor position estimation of an interior permanent-magnet synchronous machine using carrier-frequency injection methods," *IEEE Transactions on Industry Applications*, vol. 41, no. 1, pp. 38–45, 2005.

[9] M. Mamo, K. Ide, M. Sawamura, and J. Oyama, "Novel rotor position extraction based on carrier frequency component method (CFCM) using two reference frames for IPM drives," *IEEE Transactions on Industrial Electronics*, vol. 52, no. 2, pp. 508–514, 2005.

[10] H.-W. Gao, Y.-J. Yu, F. Chai, and S.-K. Cheng, "Position sensorless control of interior permanent magnet synchronous motor based on carrier frequency component method," *Proceedings of the Chinese Society of Electrical Engineering*, vol. 30, no. 18, pp. 91–96, 2010.

[11] Y. Yu, B. Wang, C. Zhu, and S. Cheng, "Analysis of rotor position estimated error for IPMSM using carrier frequency component method," *Transactions of China Electrotechnical Society*, vol. 25, no. 12, pp. 61–66, 2010.